FUNCTION american physiological society

FUNCTION, 2023, 4(6): zqad058

https://doi.org/10.1093/function/zqad058
Advance Access Publication Date: 6 October 2023
Original Research

RESEARCH ARTICLE

Breathing and Oxygen Carrying Capacity in Ts65Dn and Down Syndrome

Lara R. DeRuisseau [1,*], Candace N. Receno [2], Caitlin Cunningham [3], Melissa L. Bates [4], Morgan Goodell [5], Chen Liang [6], Brianna Eassa [7], Jessica Pascolla [1], Keith C. DeRuisseau [1]

[1]Department of Basic Sciences, University of Health Sciences and Pharmacy, St. Louis, MO 63110, USA, [2]Department of Exercise Science and Athletic Training, Ithaca College, Ithaca, NY 14850, USA, [3]Department of Statistics, Mathematics and Computer Science, Le Moyne College, Syracuse, NY 13214, USA, [4]Departments of Health and Human Physiology, Internal Medicine, and the Stead Family Department of Pediatrics, University of Iowa, Iowa City, IA 52242, USA, [5]Lake Erie College of Osteopathic Medicine, Elmira, NY 14901, USA, [6]Department of Pharmacology and Physiology, University of Rochester Medical Center, Rochester, NY 14642, USA and [7]Department of Biological Sciences, Le Moyne College, Syracuse, NY 13214, USA

*Address correspondence to L.R.D. (e-mail: Lara.DeRuisseau@uhsp.edu)

Abstract

Individuals with Down syndrome (Ds) are at increased risk of respiratory infection, aspiration pneumonia, and apnea. The Ts65Dn mouse is a commonly used model of Ds, but there have been no formal investigations of awake breathing and respiratory muscle function in these mice. We hypothesized that breathing would be impaired in Ts65Dn vs. wild-type (WT), and would be mediated by both neural and muscular inputs. Baseline minute ventilation was not different at 3, 6, or 12 mo of age. However, V_T/T_i, a marker of the neural drive to breathe, was lower in Ts65Dn vs. WT and central apneas were more prevalent. The response to breathing hypoxia was not different, but the response to hypercapnia was attenuated, revealing a difference in carbon dioxide sensing, and/or motor output in Ts65Dn. Oxygen desaturations were present in room air, demonstrating that ventilation may not be sufficient to maintain adequate oxygen saturation in Ts65Dn. We observed no differences in arterial P_{O2} or P_{CO2}, but Ts65Dn had lower hemoglobin and hematocrit. A retrospective medical record review of 52,346 Ds and 52,346 controls confirmed an elevated relative risk of anemia in Ds. We also performed eupneic in-vivo electromyography and in-vitro muscle function and histological fiber typing of the diaphragm, and found no difference between strains. Overall, conscious respiration is impaired in Ts65Dn, is mediated by neural mechanisms, and results in reduced hemoglobin saturation. Oxygen carrying capacity is reduced in Ts65Dn vs. WT, and we demonstrate that individuals with Ds are also at increased risk of anemia.

Submitted: 11 August 2023; **Revised:** 29 September 2023; **Accepted:** 3 October 2023

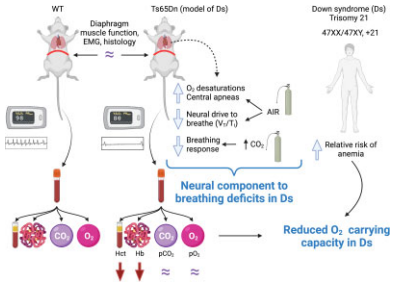

Key words: plethysmography; hypoxemia; apnea; ventilation; trisomy 21; diaphragm; hypercapnia; hypoxia

Key Points

- Down syndrome (Ds) is caused by triplication or translocation of chromosome 21 and results in intellectual disability.
- Individuals with Ds have other co-morbidities that influence their quality of life, including breathing disturbances.
- The brain of the Ts65Dn mouse has been well-characterized and Ts65Dn is used in many preclinical studies of Ds.
- We studied breathing at 3, 6, and 12 mo of age in Ts65Dn and WT.
- Ts65Dn had reduced V_T/T_i, increased central apneas, and an attenuated response to hypercapnia.
- Oxygen desaturations were more common, and hemoglobin and hematocrit were lower in Ts65Dn.
- In the medical record review, Ds had a higher relative risk of anemia.
- Diaphragm muscle function, electromyography, and histology were not different between Ts65Dn and WT.
- We conclude that Ts65Dn has an altered pattern of breathing and there is justification to continue studying mechanisms of respiratory output in Ds.

Introduction

Down syndrome (Ds) is the most common genetic cause of intellectual disability (1 in 600–800 live births).[1,2–4] In >95% of cases, Ds results from triplication of chromosome 21 while the remaining cases are due to abnormalities associated within the same chromosome.[5] Persons with Ds present with specific craniofacial features and cognitive deficits along with a spectrum of co-morbidities that can include: enlarged/protruding tongue, cardiovascular abnormalities, thyroid disease, obesity, hypotonia, upper airway obstructions, and breathing difficulties (eg, sleep apnea; SA).[6,7] Pulmonary complications are a major cause of emergency department visits for children with Ds[8] and respiratory failure is a primary factor for mortality when compared to the general population.[9] Determining mechanisms of respiratory morbidity and mortality in Ds would have important clinical impact.[10]

Respiratory infections and aspiration pneumonia routinely account for nearly 30% of Ds-related mortality.[11,12] Macroglossia, enlarged adenoids and tonsils, increased airway secretions, weakening of the respiratory muscles, and a narrowed oropharynx and trachea are hypothesized to contribute to the increased risk of lung infection and pneumonias.[13–16] Infants with Ds have more hypoxemias throughout the day compared to infants without Ds,[17] demonstrating that intermittent hypoxemia is present at early life stages in Ds. Maximal inspiratory and expiratory pressures, forced vital capacity, and forced expiratory volume in the first second (FEV_1) are lower in individuals with Ds,[18,19] indicating that respiratory muscle weakness may contribute to respiratory deficits beyond alterations in airway structure.[20] Individuals with Ds have reduced exercise capacity that may be related to respiratory muscle weakness.[21,22] During sleep, apnea is common in Ds and persists following tonsil and adenoidectomy, suggesting that obstructions are not sufficient to explain interrupted air flow during sleep in Ds.[23–25] Central apneas have been confirmed in adults with Ds[26] indicating that some apneas are neurally mediated (ie, not purely obstructive). Therefore, impairments in ventilation in Ds are likely to be multifactorial including potential reduced neural activation and/or muscular contraction.

A critical barrier to understanding and treating respiratory impairments and disease in Ds is the availability of an appropriate model to answer such questions. Respiratory parameters are challenging to measure in persons with Ds, which may explain the small number of studies characterizing resting, eupneic breathing, and respiratory muscle strength in this population.[18,19,27] The Ts65Dn mouse has been used for multiple mechanistic studies in Ds, including preclinical trials.[28–30] Oxygen saturation is reduced in these mice compared to wild-type (WT) mice.[31] Determining the respiratory phenotype and its mechanistic underpinnings in this model of Ds is an important step in informing future studies of respiratory comorbidities.

We aimed to characterize the pattern of breathing in conscious 3, 6, and 12-mo-old Ts65Dn and WT disomic male mice exposed to air, hypoxia, and hypercapnia. Our overarching hypothesis was that Ts65Dn mice would have impaired breathing caused by neural and muscular components. Ds is both neurodevelopmental and neurodegenerative, and considered to have accelerated aging. Therefore, we also hypothesized that this phenotype would worsen with advancing age. To quantify the contribution of potential respiratory impairment on hematological outcomes and oxygen carrying capacity, we quantified arterial blood gases, hemoglobin concentration and hematocrit levels, and arterial O_2 saturation in awake mice breathing room air. Electromyography, in-vitro muscle function and fiber type quantification were performed on the diaphragm. Finally, given limited human evidence in the literature, we performed a retrospective medical record review to determine if our hemoglobin and hematocrit findings were borne out in a human population with Ds.

Methods

Ethical Approval

Ts65Dn and colony control WT male mice were delivered from The Jackson Laboratory (stock #005252);[32,33] and aged to 3, 6, and 12 mo of age ($n = 47$ total that survived to the age points).

Additional mice were added to the pulse oximetry experiments ($n = 17$). Once arriving to the facility, mice were implanted with the LifeChip system (Destron Fearing, Airport, TX). The microchip ID was used to blind all experimenters involved directly with data collection. Mice were kept on a 12-h light and 12-h dark cycle, ~24°C housing temperature, group housed in a room with only males, and fed *ad libitum* with standard rodent chow (Harlan, Teklad 2215 Rodent Diet 8640) and constant access to water. All data were collected during the light cycle. A subset of breathing data from WT mice have been published in a study on the collection of baseline data in young- and middle-aged mice.[34] All procedures were approved by the Le Moyne College Institutional Animal Care and Use Committee (2016-01). Le Moyne College holds a Domestic Animal Welfare Assurance (D17-00947) through the Office of Lab Animal Welfare at the National Institutes of Health. Human data were extracted from the TriNetX platform, which reports deidentified patient data in aggregate. The use of this platform has been deemed to be exempt from review by the Institutional Review Board at the University of Iowa.

Experimental Design

Unrestrained barometric plethysmography and pulse oximetry were performed on conscious mice at 3, 6, and 12 mo of age. These ages were selected to correspond with young- (3 mo), adult- (6 mo), and middle-age (12 mo) mice, similar to other reports of mouse behavior.[35,36] Terminal experiments including conscious arterial blood sampling, EMG, in-vitro diaphragm muscle function, and diaphragm muscle fiber typing were performed on mice aged 13 mo.

Barometric Plethysmography

Experiments were performed between 4 and 7 h after the start of the light cycle with 1 mouse tested at a time as previously described.[37] Buxco mouse chambers were used with the reference chamber and animal chamber attached via SMC Soft-polyurethane tubing (Model TUS 0604 Y-20) to the ports of a Validyne transducer (DP45 Transducers) for monitoring of pressure changes. The Validyne voltage output was signal conditioned (ACQ 7700) and further analyzed with Ponemah software (DSI) using the Drorbaugh and Fenn equation for tidal volume.[38] The barometric plethysmography system was calibrated prior to each use. Flow for each chamber was held at ~300 mL/min using a mixture of nitrogen, oxygen, and carbon dioxide from pressurized canisters (Purity Plus Specialty Gases Grade 5.0 ultra pure) that were mixed with a 3 channel gas blender (MCQ Instruments, GB-103). This amount of flow prevented elevated levels of CO_2 throughout the experiment. Flow was measured prior to entering the bias flow opening on the mouse chambers using TSI 4100 Series Flowmeters (Shoreview, MN) that had been factory calibrated within 1 yr. Each chamber was equipped with a humidity and temperature probe that was incorporated into the Ponemah software for calculation of tidal volume and minute ventilation. A barometric pressure probe monitoring the room was connected to the ACQ 7700 signal conditioner and Ponemah software. Metabolic sensing was performed as previously described[39] using a CD-3A AEI metabolic analyzer (Pittsburgh, PA). Following data collection, breaths were analyzed offline using Ponemah (analysis software service pack version 4.0 and 5.0) review mode to quantify breathing frequency, tidal volume, inspiratory time, minute ventilation, apneas, augmented breaths, and V_{CO2}.[40]

Animal Testing

After calibration of the system, mice were placed into the barometric plethysmography chamber receiving ~300 mL/min of pressurized air (20.93% oxygen [O_2], balanced nitrogen [N_2]; mixed with MCQ Instruments, GB-103) with a vacuum of 100 mL/min from the chamber. Baseline was identified as quiet breathing when mice appeared awake, calm, and conscious (had minimal movement within the chamber, but eyes were open and appeared to be awake). This typically took 1–2 h to achieve. After baseline with air, mice were exposed to a hypoxic challenge (10% O_2, balance N_2) for 10 min, then a 10-min recovery period with air, followed by 10 min of hypercapnia (5% CO_2; balance air), and another 10-min recovery period with air. Throughout the experiment, body temperature was measured using the LifeChip system (Destron Fearing, Airport, TX) to identify any possible shifts of more than 1°C. If temperature changed by >1°C, the new temperature was entered into the software for re-calculation of V_T. We rarely observed a change of body temperature and this finding could be due to the warmer ambient temperature of ~24°C of the experiments.

Metabolic Sensing

Due to the higher flow used in the barometric plethysmography set-up, we performed metabolic testing in a separate series of experiments. Based on preliminary testing, we brought the inflow to 120 mL/min; this allowed adequate sensitivity of CO_2 and O_2 measurements. We were not able to do the lower flow experiments in the 6-mo group. After calibration, mice were allowed to acclimate 50–60 min and then a sample was drawn through AEI metabolic analyzers (Pittsburgh, PA; CD-3A) and a 10-min average was calculated as previously described.[34,40]

Pulse Oximetry

Pulse oximetry was performed after breathing measurements. Some additional mice were used for pulse oximetry experiments that did not undergo barometric plethysmography. Under isoflurane anesthesia, depilatory cream was applied to the neck for removal of fur where the pulse oximetry collar would be located. After >1 d recovery from fur removal, mice were placed in a testing chamber with the pulse oximetry collar in place (Starr Life Sciences, Oakmont, PA). Typical bedding, food, and water were accessible during the testing protocol. Mice were followed for collection of oxygen saturation, while breathing room air for 1 h. If necessary, the collar was adjusted during the session to allow for adequate signal transmission. Data were only used if all measures were accepted by the software (no errors). Instances of desaturation were defined as ≤ 5 s bouts of ≤ 85% oxygen saturation documented by the software and counted for the last hour of the pulse oximetry protocol.

Arterial Blood Sampling

Thirteen-month-old male mice were utilized in the blood sampling experiments. Anesthesia induction was performed with 3% isoflurane at a flow rate of 500–800 mL/min, followed by anesthetic maintenance using a nose cone with 2%–2.5% isoflurane at the same flow rates. Before beginning the surgery, depth of anesthesia was confirmed and eye protectant administered. A far infrared heating platform (Kent Scientific) was utilized throughout the procedure for animal warming. Fur was removed and alcohol and betadine scrub was used to clean the surgical site. An incision was made and the tissue reflected to view

the femoral artery. The artery was isolated and ligated distally, while the proximal end was clamped with a Roboz 2A butterfly clamp (RS-6472, Gaithersburg, MD). A 30 gauge needle bent at 90° punctured the artery and the catheter was placed into the artery and tied down. Following removal of the clamp, the catheter was advanced and tied at another point. Catheters were made by joining a PE-10 tube (pulled on one end) to a PE-50 tube. All catheters were filled with sterile saline prior to surgery.

Once the catheter was tied in place, a plug was inserted into the end of the catheter and the incision was sutured closed. Lidocaine (placed along the incision) and Rimadyl (10 mg/kg; subcutaneously) were administered for analgesia and pain management. Mice were allowed to recover in their cage for 45–90 min prior to taking 0.1–0.13 mL arterial blood. Samples were only initiated if mice had body temperature ~37°C, were eating, ambulating, and appeared overall to be recovered from the anesthesia. All blood samples were collected into a 1 mL syringe and transferred into a CG8 + I-STAT cartridge for measuring P_{aCO2}, P_{aO2}, pH, hemoglobin, and hematocrit. After the arterial sample, mice were re-anesthetized with isoflurane for electromyography followed by euthanasia.

Electromyography

Mice (13 mo of age) were anesthetized to a surgical plane of anesthesia using 3% isoflurane for induction followed by ~2% maintenance with a nose cone. A stainless steel wire (0.008 coated; A–M Systems, Carlsborg, WA) was inserted via a needle through the skin, underneath the last rib into the diaphragm. Electromyography (EMG) signals were amplified at a gain of 500, filtered between 10 Hz and 1 kHz using an analog amplifier (Model 3000 Differential AC/DC Amplifier, A–M Systems). They were digitized at 2 kHz and recorded (IWX/214, iWorks, Dover, NH) with the recording period lasting at least 60 s, at which time isoflurane was reduced to 1.5% while maintaining a surgical plane of anesthesia. EMG amplitude was estimated using root-mean-squared (RMS) EMG over a 50-ms moving window (LabScribe). As other groups have observed, RMS EMG correlates with force in diaphragm.[41,42] RMS EMG was quantified from 1-min recording sessions and averaged to obtain the single values for each animal, respectively.

In-Vitro Diaphragm Muscle Function

Diaphragm muscle function was measured in mice as previously described,[43,44] following the EMG protocol. This procedure is terminal. Isoflurane was brought back to 3%, surgical depth of anesthesia was re-confirmed, and the diaphragm was removed and placed in a bath containing Krebs–Henseleit buffer and a 95%O_2/5%CO_2 gas. After removal of the diaphragm, the heart was excised to confirm euthanasia. A muscle strip cut along parallel fibers was clamped horizontally in a DMT myograph system (820 M, Denmark) bath containing a Krebs–Henseleit buffer and 95%O_2/5%CO_2 and secured using the ribcage and central tendon attachments. After a 15-min equilibration at 37°C, the contractile protocol began. The diaphragm strip was stimulated at supramaximal stimulation voltage (~150%) while determining optimal length (L_0). The length of the muscle was gradually increased and stimulated with single twitches until L_0 was determined. Once this occurred, muscle was stimulated at this optimum length for maximal twitch and tetanic tension (120 Hz, 500 ms trains) production. Force–frequency response was measured at 1–300 Hz (500 ms trains), separated by 3 min between stimulations. After force–frequency, strips recovered for 5 min before undergoing a 30-min fatigue protocol (30 Hz, 250 ms trains). Recovery was also recorded for the 15 min immediately following fatigue. The % initial force from baseline was calculated at 1, 5, 10, 15, 20, 25, and 30-min time points of the fatigue protocol, as was % recovery for 30 s, 1, 2, 5, 10, and 15-min time points. Force production (P_0) was calculated and normalized to diaphragm strip cross sectional area (cm^2).

Myofiber Cross-Sectional Area and Distribution

Diaphragm muscle was obtained from anesthetized mice. A strip of diaphragm was sectioned, positioned in Tissue-Tek O.C.T. and allowed to settle to an unstressed length prior to freezing in liquid nitrogen cooled isopentane. Frozen samples were stored at −80°C. This method of standardizing fiber bundle length between samples has been published[45,46] and shown to be a reliable method to standardize diaphragm muscle length for cross-sectional area (CSA) measurements. Sections were cut at 10 μm using a cryostat, mounted on glass slides, air dried, followed by incubation in phosphate-buffered saline (PBS) containing 0.5% Triton X-100. Sections were rinsed in PBS and simultaneously incubated with antibodies directed against dystrophin (~50 μL), myosin heavy chain type I/IIa and type IIb (BF-F3 and BF-35; DSHB, IA) in a dark humid chamber at RT for 1 h. Sections were washed with PBS, incubated with TRIT-C goat anti-rabbit IgG (1:10) (Invitrogen, Carlsbad, CA), DAPI goat anti-mouse IgM (1:10) and FITC goat anti-mouse IgG (1:10) antibodies diluted in 10% normal goat serum in PBS in a dark humid chamber at RT for 1 h. Sections were washed 3x in PBS and mounted with DAPI Vectashield mounting medium (Vector Laboratories, Burlingame, CA), coverslipped, and sealed for viewing. Images were obtained at 10× magnification using a Zeiss AxioImager fluorescence microscope equipped with an AxioCam MRc digital camera and analyzed with AxioVision software. Myofiber CSA (μm^2) was determined on a maximum of 300 fibers, averaging 290 type I/IIa fibers, 189 type IIx, and 46 type IIb fibers. Dystrophin was labeled red, type I/IIa fibers green, type IIx unstained, and type IIb blue. Fiber type proportion was determined from counts of type I/IIa, type IIx, and type IIb fibers and expressed as a percentage of the total number of fibers.

Retrospective Medical Record Review

The retrospective medical record review was performed using the TriNetX platform, which aggregates deidentified data from 58 healthcare organizations. A cohort of Ds patients was created from ICD-10 codes for Ds (Q90) and billing codes for an encounter. A control cohort was built by excluding the ICD-10 code for Ds. Case-control matching was performed for age at first encounter and race. Incidences of anemia were then extracted using ICD-10 codes for aplastic anemias (D60–D64), nutritional anemias, including iron deficiency (D50–D53), and hemolytic anemias (D55–D59).

Statistics

Baseline breathing was analyzed by ANCOVA (analysis of covariance) with body weight as a covariate. For the hypoxia and hypercapnia exposures, a *functional t*-test analysis was performed at each age group across the 10 min of gas challenge. Functional analysis assumes that there is an underlying curve

Table 1. Average Baseline Breathing Measures in WT and Ts65Dn Mice

Age	Type	Frequency (bpm)	V_T (mL/breath)	V_T/g body weight ([mL/breath/g]*10^3)	V_E (mL/min)	V_E/g body weight (mL/min/g)	Body Weight (g)	V_T/T_i (mL/s)
3 Mo	WT	154 ± 22	0.37 ± 0.10	10.2 ± 4.25	58.3 ± 20.5	1.60 ± 0.78	38.4 ± 7.5	2.79 ± 0.98
	Ts	152 ± 33	0.36 ± 0.17	10.5 ± 5.03	53.5 ± 25.5	1.55 ± 0.72	34.7 ± 5.3	*1.88 ± 0.53
6 Mo	WT	150 ± 15	0.41 ± 0.18	11.5 ± 4.03	54.8 ± 13.0	1.71 ± 0.54	35.2 ± 3.7	2.16 ± 1.25
	Ts	132 ± 38	0.36 ± 0.07	12.2 ± 2.60	43.4 ± 8.5	1.54 ± 0.16	29.4 ± 1.9	*1.63 ± 0.75
12 Mo	WT	157 ± 19	0.47 ± 0.06	9.55 ± 0.88	‡70.3 ± 12.1	1.50 ± 0.22	45.7 ± 3.0	3.11 ± 0.80
	Ts	146 ± 56	0.50 ± 0.16	13.6 ± 3.89	‡67.3 ± 18.1	1.90 ± 0.79	37.0 ± 6.8	*2.39 ± 0.95

Frequency (bpm), tidal volume (V_T; mL/breath), minute ventilation (V_E; mL/min), tidal volume to inspiratory time ratio (V_T/T_i; mL/sec) during baseline room air (20.93% O_2; balanced N_2) breathing in WT and Ts mice. Mice were tested at 3 mo ($n = 7$ WT, $n = 8$ Ts), 6 mo ($n = 7$ WT, $n = 7$ Ts), and 12 mo ($n = 11$ WT, $n = 7$ Ts) of age. Frequency and V_T were not significantly different between groups ($P > .05$). An age effect was identified for V_E (‡$P = .047$; age effect). Strain differences emerged for V_T/T_i, where V_T/T_i was significantly lower in Ts mice (*$P = .021$). Data were analyzed using ANOVA and presented as mean ± SD.

over time for each subject that we are observing at only specific time points. To perform functional analysis, we first estimate the underlying curve for each subject and then calculate the average curve over time for each group. The functional *t*-test then looks for specific intervals where the 2 mean curves for the groups are statistically different from each other. Unlike a repeated measures analysis, which can only identify specific timepoints as being different, because the functional *t*-test estimates the curve across the entire timepoint, it can give continuous intervals where we can conclude differences exist.[47]

Since apneas are count data, a Poisson regression was used to analyze this data set. Poisson regression is appropriate when nonequal variances and non-normality occur, but assumes equal means and SD by group (an assumption that is met with these data). Augmented breaths were analyzed with a 2-way ANOVA to examine the effect of age and strain. The assumptions of equal variance and normality were tested and met. Because of the un-equal group sizes, Type III sum of squares was used to assess significance for augmented breaths. Desaturations are count data, which would usually be modeled with Poisson regression. However, that analysis has the requirement of approximately equal mean and SDs, which is not met with these data. For this reason, Negative Binomial Regression was used to analyze desaturation count data. Arterial blood sampling, muscle fiber typing, and EMG data were analyzed using independent sample *t*-tests with Bonferonni used for post-hoc analysis when appropriate. Diaphragm muscle function was analyzed with a 2-way ANOVA using strain and time/hertz as the groups. Relative risk was calculated for outcomes from the retrospective record review and difference in relative risk was analyzed by Z-test. Significance was selected a priori at $P < .05$. R software and Prism were used to perform statistical analyses.

Results

Baseline Breathing Characteristics

Baseline, eupneic breathing data are presented in Table 1. V_T/T_i was lower for Ts65Dn vs. WT (strain effect; $P = .021$), suggesting a lower neural drive to breathe.[48] Breathing frequency, tidal volume, and minute ventilation were not different between strains, although an age effect (only; no strain or age by strain interaction) was detected ($P = .047$) for minute ventilation. V_E/V_{CO2} was higher (strain effect; $P < .001$) in Ts65Dn vs. WT (3 mo: Ts 5.19 ± 2.87 vs. WT 2.78 ± 1.35 mL/min/g; 12 mo: Ts 4.72 ± 2.25 vs. WT 2.81 ± 1.01 mL/min/g) driven by the lower V_{CO2} in Ts65Dn mice.

Hypoxia and Hypercapnia Exposure

Breathing data at baseline and during 10 min of hypoxia (10% O_2) and hypercapnia (5% CO_2) are presented in Figure 1. The hypercapnic V_E response was attenuated in Ts65Dn mice at 12 mo. While all mice had increased V_E, breathing frequency, and V_T in response to hypoxia and hypercapnia, Ts65Dn mice had a significantly blunted ventilatory response to hypercapnia that was age dependent. Twelve-month-old Ts65Dn mice had a reduced V_E response in both of our statistical analyses: (1) when comparing minute by minute raw data ($P = .03$) and (2) when each minute was subtracted from the air breathing baseline (relative difference to baseline; $P = .015$). At 3 mo, the overall breathing frequency response to hypercapnia (data not shown) was lower for Ts65Dn vs. WT with both statistical analyses: (1) the minute by minute raw data ($P = .02$) and (2) when each minute was subtracted from the air breathing baseline (relative difference to baseline; $P = .02$). V_T (data not shown) was lower for Ts65Sn vs. WT at 12 mo only when each minute was subtracted from the baseline (relative difference to baseline; $P = .02$).

Apneas and Augmented Breaths

Apneas (lack of flow ≥ 0.5 s) and augmented breaths were quantified during air breathing in WT and Ts65Dn (Figure 2). Apneas observed through barometric plethsmography with zero flow fluctuations are due to a lack of respiratory effort, which is a direct physiological measure of a centrally mediated breathing deficit.[49,50] Strain ($P < .001$) and age ($P < .001$) effects, and a strain × age interaction ($P < .001$) were detected for apneas, with fewer apneas in WT mice. Three-month-old Ts65Dn mice had fewer apneas than 6 and 12 mo mice ($P < .0001$), but there was no difference between 6- and 12-mo-old Ts65Dn mice. Six-month-old WT mice had more apneas than 3 and 12 mo mice ($P < .0001$ for both comparison), but there was no difference between 3 and 12 mo mice. Ts65Dn mice had more apneas than WT at every age ($P < .0001$), with the largest difference observed at 12 mo. Augmented breaths were not different between strains, although an age effect ($P = .002$; Figure 2) was observed with fewer augmented breaths detected in older mice. For augmented breaths, we observed that 3-month-old was higher than 6 mo ($P = .0206$) and 12 mo ($P = .003$), but there is no statistical difference between 6 and 12 mo.

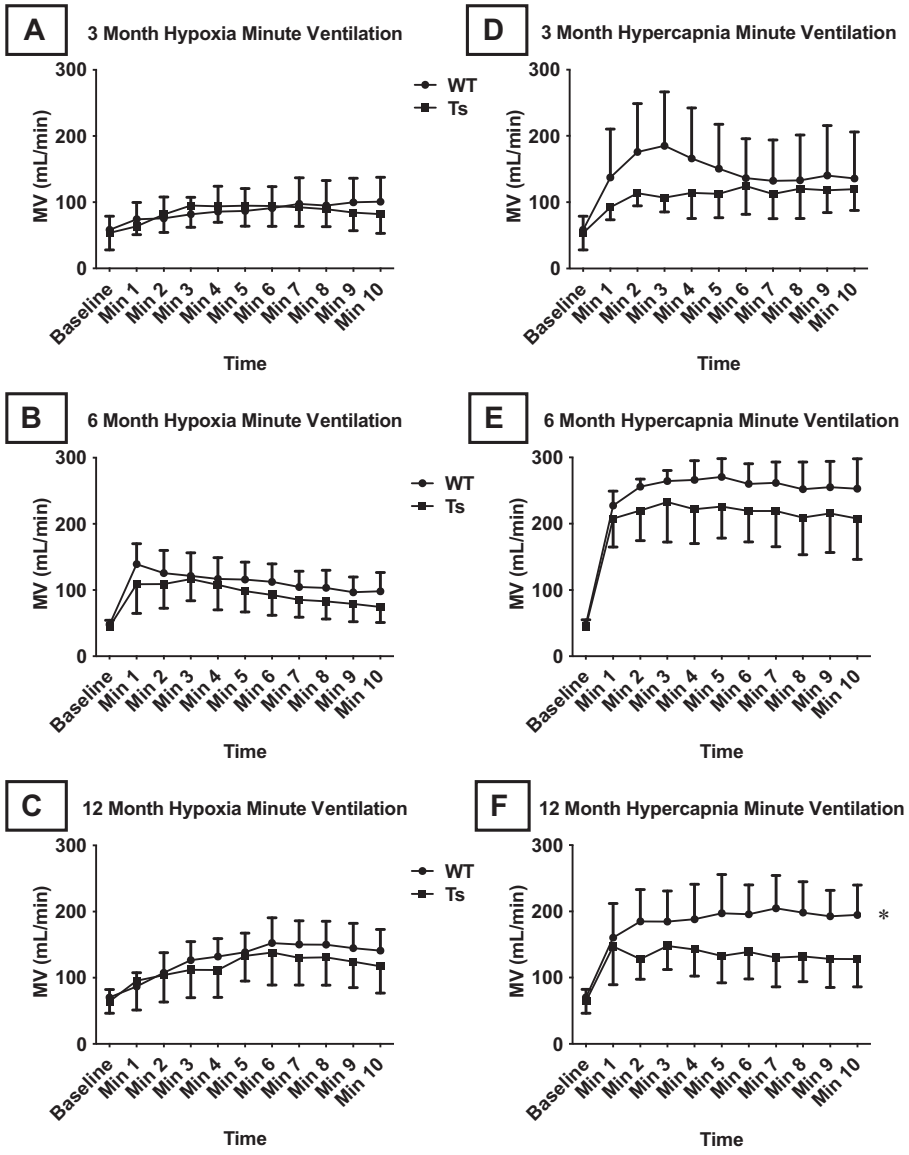

Figure 1. Minute ventilation during baseline and 10 min of hypoxia and hypercapnia. Average minute ventilation (mL/min) for baseline (room air: 20.93% O_2; balanced N_2) and minute by minute response to 10% hypoxia (10% O_2; balanced N_2) was measured in (**A**) 3 mo wild-type (WT) mice ($n = 7$) and Ts65Dn (Ts) mice ($n = 8$), (**B**) 6 mo WT mice ($n = 7$) and Ts mice ($n = 7$), and (**C**) 12 mo WT mice ($n = 11$) and Ts mice ($n = 7$). Following a 10-min recovery, minute by minute response to 5% hypercapnia (5% CO_2; 20.93% O_2; balanced N_2) was measured in the same (**D**) 3 , (**E**) 6, and (**F**) 12 mo WT and Ts mice. Hypercapnic exposure revealed a strain difference, but only at 12 mo where Ts mice showed a lower MV response (*$P = .03$ raw/absolute values, $P = .015$ vs. baseline) compared to WT counterparts. No significant differences were detected in response to hypoxia ($P > .05$).

Desaturations

The number of desaturations ($SaO_2 < 85\%$ for up to 5 s) in freely moving mice were counted over 1 h in the light cycle (Figure 3). There was a main effect for strain ($P = .03$), with WT having fewer desaturations compared to Ts65Dn mice. There was also an overall age effect ($P = .045$), 3 mo was higher than 12 mo ($P = .011$).

Conscious Arterial Blood Sampling

Conscious arterial blood sampling was performed in 13-mo-old mice (Figure 4). Hemoglobin ($P = .025$) and hematocrit ($P = .023$) were higher in WT vs. Ts65Dn mice. All other arterial blood variables were similar between groups, including P_{aO2} and P_{aCO2}.

Diaphragm Electromyography

Diaphragm EMG was performed in 13-mo-old mice (Figure 5). Electromyography amplitude was estimated using RMS EMG. Root-mean-squared was similar between WT and Ts65Dn ($P > .05$).

In-Vitro Diaphragm Function

There was no difference between groups in the tetanic, twitch, or diaphragm force frequency response ($P > .05$; Figure 6A and B) and the reported values are in line with previous reports.[43,51–53] Fatiguing contractions led to an expected decrease in muscle force production expressed as % initial force. No differences in muscle force were observed between groups during 30 min of

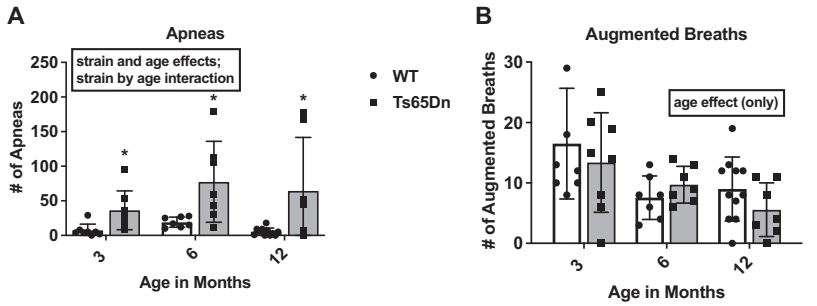

Figure 2. Apneas and augmented breaths in conscious mice. (**A**) Apneas (lack of flow ≥ 0.5 s) and (**B**) Augmented Breaths for WT mice ($n = 26$) and Ts65Dn mice ($n = 22$) over 30 min breathing air. Apneas and augmented breaths were determined over 30 min. Apneas were defined as periods of suspended breathing lasting > 0.5 s, and augmented breaths were indicated by a sharp rise in the breathing trace above 1.25 mL/s followed by a sharp decrease below −0.75 mL/s. Strain ($P < .001$), age ($P < .001$), and a strain by age interaction ($P < .001$) were detected for apneas, with fewer apneas in WT mice. Augmented breaths were not different between strains, although an age effect ($P = .002$) was observed with fewer augmented breaths detected in older mice.

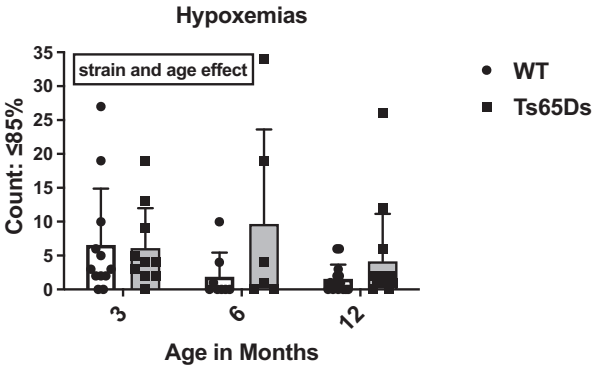

Figure 3. Hypoxemias in conscious mice. The MouseOx pulse oximeter was used to detect oxygen saturation over 1 h of room air breathing. Oxygen saturation below 85% for up to 5 s was counted as 1 hypoxemia in WT ($n = 34$) mice and Ts65Dn ($n = 30$). A strain ($P = .03$) and age effect ($P = .045$) were detected.

fatiguing contractions ($P > .05$; Figure 6C) or 15 min of recovery ($P > .05$) (Figure 6D).

Diaphragm Muscle Fiber CSA and Distribution

Diaphragm skeletal muscle histology is presented in Figure 7. Mean CSA values for type I/IIa, type IIx, and type IIb are shown in Figure 7A. No significant differences ($P > .05$) were detected in the CSA of any fiber type between groups. Type I/IIa, IIx, and IIb fiber were counted and expressed as a percentage of the total number of muscle fibers on the section and shown in Figure 7B. No difference was observed ($P > .05$) in the muscle fiber distribution between groups. Representative images of diaphragm obtained from Ts65Dn and WT mice are shown in Figure 7C and D. Regarding the reported fiber CSA values, while the current data are comparable to values published by other groups,[54–57] the method we utilized to standardize fiber CSA may have contributed to our values being larger than reported values when diaphragm is stretched to optimum muscle length.[58,59] Thus, the importance of specifying the method utilized to standardize fiber bundle length prior to sectioning should be specifically described as it may impact interpretation of CSA values.

Retrospective Record Review

Two groups of control ($n = 52$ 346, 16 ± 18 y) and Ds ($n = 52$ 346, 16 ± 19 y) patients were identified and matched by age (Table 2). Because of the large cohort size, we detected a statistically significant difference in age ($P = .04$), although there is likely little

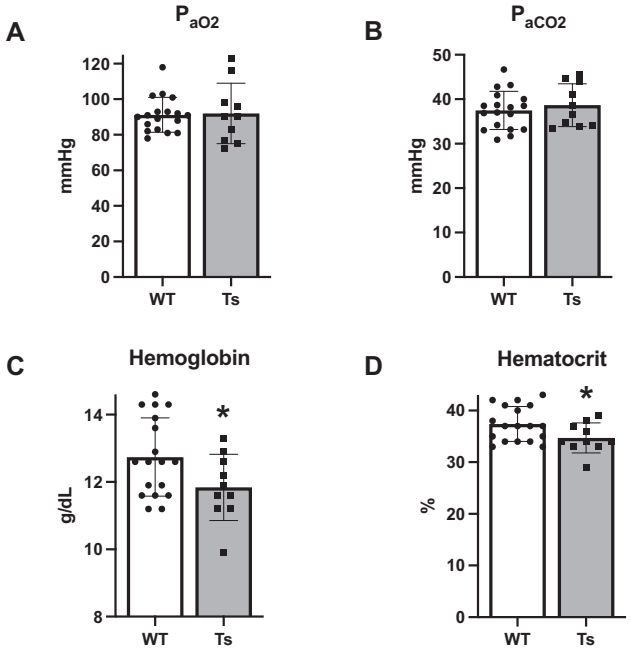

Figure 4. Arterial blood sampling in conscious mice. (**A**) Partial pressure of oxygen (P_{aO2}), (**B**) partial pressure of carbon dioxide (P_{aCO2}), (**C**) hemoglobin, and (**D**) hematocrit for WT mice ($n = 18$) and Ts65Dn ($n = 10$). Mice were implanted with a femoral catheter under a plane of anesthesia and allowed to recover. Once mice were ambulating throughout the cage and eating, a sample was collected in awake mice breathing room air. There were no significant differences for P_{aO2} ($P = .896$) or P_{aCO2} ($P = .516$) between groups. Hemoglobin (Hb) and hematocrit (Hct) were different. One mouse was removed due to Hb and Hct levels > 3 SD from the mean.

physiological impact of the < 1 y age difference between groups. Relative risk for the Ds group was higher for nutritional anemia, hemolytic anemia, and aplastic and other anemias ($P < .0001$ all comparisons).

Discussion

This investigation studied breathing behavior, hematological outcomes, and diaphragm muscle function in Ts65Dn and WT mice and utilized a retrospective medical record review to confirm unique hematological findings. During exposure to air, breathing frequency, tidal volume, and minute ventilation were similar at 3, 6, and 12 mo of age. However, apneas were elevated and V_T/T_i was decreased in Ts65Dn, demonstrating a

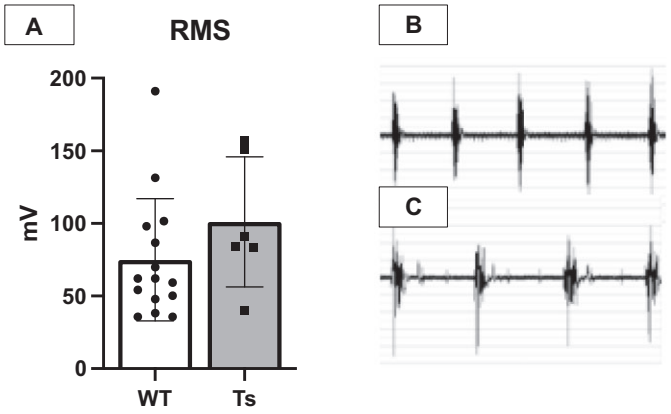

Figure 5. Diaphragm EMG in anesthetized mice. (**A**) Root-mean-squared (RMS) EMG amplitude for WT mice ($n = 15$) and Ts65Dn ($n = 6$) and a raw signal for a (**B**) WT mouse and (**C**) Ts65Dn mouse. Mice were anesthestized with isoflurane and a fine wire was inserted into the diaphragm. Electromyography signals were amplified at a gain of 500, filtered between 10 Hz and 1 kHz using an analog amplifier (Model 3000 Differential AC/DC Amplifier, A–M Systems). Data were collected and averaged over 1 min. There were no significant differences for RMS EMG ($P = .112$). One mouse was removed due to values > 3 SD from the mean.

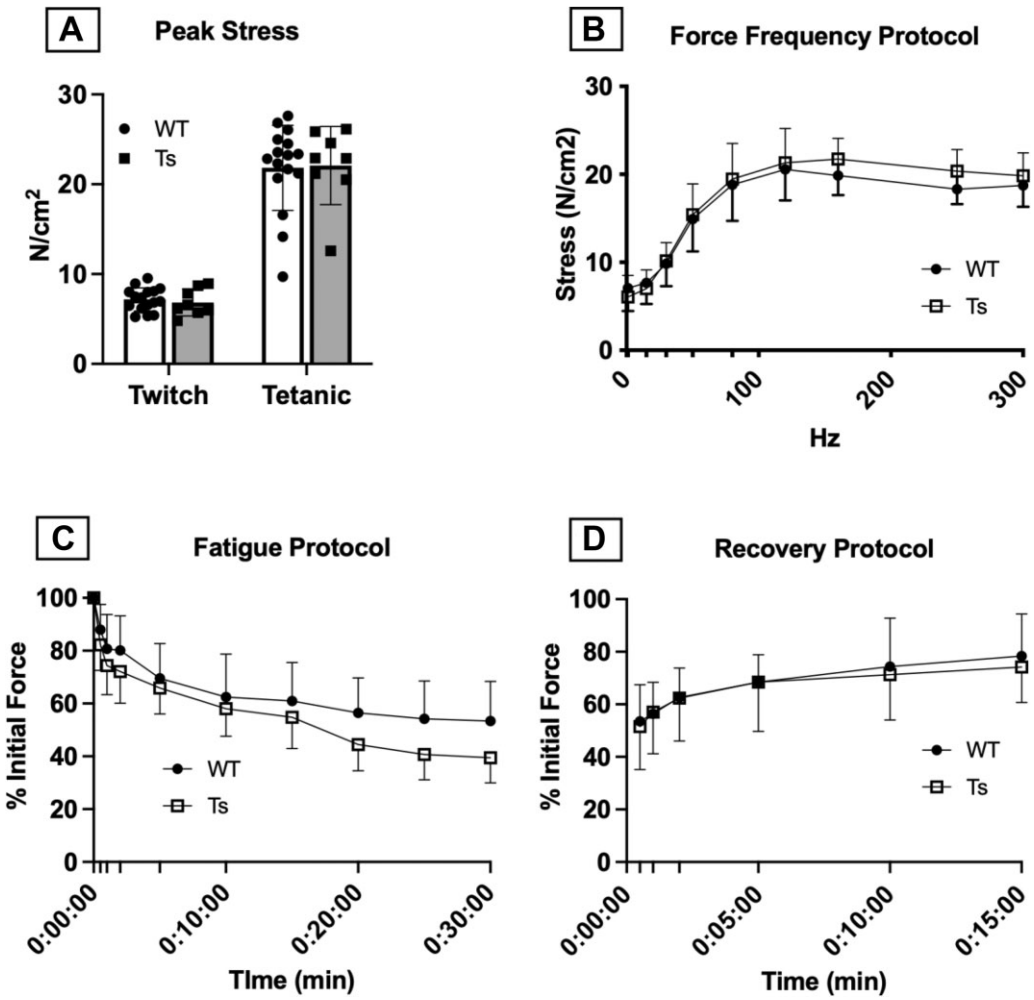

Figure 6. In-vitro diaphragm strip muscle function. (**A**) Twitch and tetanic peak-stress (N/cm^2). (**B**) Force–frequency curves expressed as a function of specific force production (N/cm^2) at simulation frequencies between 10 and 300 Hz in wild type (WT; $n = 16$) and Ts65Dn (Ts; $n = 8$) mice, (**C**) relative fatigue development of diaphragm strips from WT and Ts mice during a 30-min fatigue protocol where strips were stimulated submaximally every 2 s at 30 Hz, and (**D**) relative force recovery over 15 min immediately following the fatiguing protocol. No significant differences between groups were detected for contractile measures ($P > .05$).

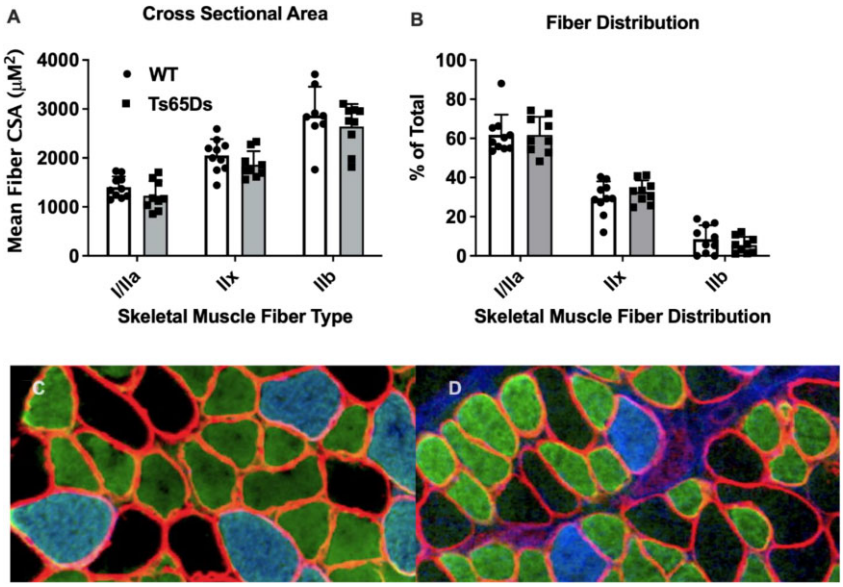

Figure 7. Diaphragm muscle histology. (**A**) Mean CSA values for type I/IIa, type IIx, and type IIb ($P > .05$). B.) Type I/IIa, IIx, and IIb fiber were counted and expressed as a percentage of the total number of muscle fibers on the section ($P > .05$). (**C**) and (**D**) Representative images of diaphragm obtained from WT (**C**) and Ts65Dn (**D**) mice.

Table 2. Relative Risk of Anemia in Ds and Control Patients With and Without Sleep Apnea

	ICD-10 Codes	Mean ± SD, %, or Relative Risk	P-Value
Control ($n = 52,346$)			
Age		16 ± 18	
Sex		49.6% Male	
White (%)		51.0%	
Ds ($n = 52,346$)	Q90		
Age		16 ± 19	.04
Sex		64.7% Male	<.0001
White (%)		51.6%	<.001
Nutritional anemias	D50–D53	3.60 (3.29, 3.94)	<.0001
Hemolytic anemias	D55–D59	1.86 (1.60, 2.17)	<.0001
Aplastic and other anemias	D60–D64	3.61 (3.36, 3.81)	<.0001
Control with sleep apnea ($n = 13,755$)	G47.3		
Age		16 ± 16	
Sex		55.4% Male	
Ds with sleep apnea ($n = 13,755$)	Q90, G47.3		
Age		16 ± 16	>.99
Sex		55.4% Male	>.99
Nutritional anemias	D50–D53	1.34 (1.19, 1.50)	<.0001
Hemolytic anemias	D55–D59	0.87 (0.70, 1.07)	.19
Aplastic and other anemias	D60–D64	1.52 (1.39, 1.66)	<.0001

Human data demonstrating relative risk of anemia in Ds from the TriNetX platform. In the entire cohort, individuals with Ds have higher relative risk of all types of anemia ($P < .0001$). When comparing only those individuals with sleep apnea, Ds has a higher relative risk of nutritional and aplastic and other anemias ($P < .0001$).

neural component to the pattern of breathing in Ts65Dn. Upon exposure to gas challenges, the Ts65Dn group showed an attenuated breathing frequency (3 mo) and V_E and V_T (12 mo) response to hypercapnia, revealing a CO_2 sensing or motor output deficit in Ts65Dn. Oxygen desaturations were greater and hemoglobin concentration and hematocrit levels were lower in Ts65Dn. In the retrospective medical record review, relative risk of anemia was higher in Ds, confirming that our findings of decreased hematocrit and hemoglobin in Ts65Dn mice have relevance to humans with Ds. Muscle fiber-typing, in-vitro muscle function and raw EMG were similar in Ts65Dn and WT. Overall, there does not appear to be a diaphragmatic muscle function component to low-force breathing behaviors at 3, 6, or 12 mo in Ts65Dn but neural contributions are present.

The increased apneas and oxygen desaturations in Ts65Dn mice are in line with reports of individuals with Ds.[60,61] Sleep apnea[62] and daytime apneas[17] are common in Ds and may contribute to other co-morbidities and executive functioning,[63,64] making it an important area of investigation to improve the lives of individuals with Ds. It should be noted we did not investigate sleep apnea per se, but we studied mechanisms that may contribute to respiratory control in this population. While most data in the literature surround apneas during sleep, there are also reports of daytime apneas in infants.[17] Although apneas during sleep were previously considered to be obstructive, removal of tonsils and adenoids does not often improve breathing in Ds,[23,24] suggesting another contributor to disordered breathing. Additionally, central sleep apneas have been observed in Ds,[26,65]

along with reports of unstable ventilatory control in children with comparable sleep apnea to typically developing children.[66] Overall, this information points to a possible neural component to breathing abnormalities in Ds. Data from this report demonstrate that Ts65Dn have central apneas, reduced V_T/T_i and an attenuated response to hypercapnia, and may be an appropriate model to further investigate respiratory physiology in Ds.

To understand neural mechanisms of breathing in Ds, we evaluated baseline breathing. While basic parameters were similar (breathing frequency, tidal volume, minute ventilation) to WT, V_T/T_i was lower in Ts65Dn, suggesting a lower neural drive to breathe.[48] There were also increased apneas in Ts65Dn during air exposure. With barometric plethysmography, a complete cessation of flow is indicative of a central apnea since an obstructive apnea results in a flow limitation with some pressure fluctuation detected in the chamber.[50] These baseline differences starting at 3 mo of age are in line with younger individuals with Ds displaying central apneas and hypoventilation.[65,66] The central apneas and reduced neural drive to breathe shows Ts65Dn display a neural component to their air breathing that is different from WT. This point is important as it reveals at baseline there is an altered breathing pattern for Ts65Dn. It is likely when they are stressed or performing other activities, that more extreme differences may emerge. In people with Ds, cardiorespiratory responses to exercise are reduced[22,67] and this finding could be due in part to CO_2 sensing and the motor response to changes in CO_2. For instance, at 3 (breathing frequency) and 12 (V_E, V_T) mo of age, we observed a reduced response to hypercapnia in Ts65Dn, which means either the CO_2 sensing, or the motor response, or both, were impaired in this group.

The observation of a blunted hypercapnic response in Ts65Dn suggests that CO_2 integration may be a contributor to disordered breathing in Ds. The higher V_E/V_{CO2} in Ts65Dn vs. WT at baseline also points to a mismatch between minute ventilation and exhaled CO_2. Although V_E is similar between strains, when normalized to the lower V_{CO2} in Ts65Dn, the V_E/V_{CO2} is higher compared to WT. While V_E/V_{CO2} is a common way to present data in the respiratory field, there is a continued discussion about ways to normalize data in Ds since the physiology is different and common risk factors do not reflect incidence in Ds.[68] Therefore, we suggest caution when interpreting normalized physiological data in Ts65Dn or Ds. It is possible these mice were in alkalosis at this point in time based on the higher V_E/V_{CO2}, although it could also highlight that typical normalizers do not appropriately reflect baseline physiology in Ts65Dn and Ds. Based on the number of apneas and desaturations measured by dips of oxygen saturation $\leq$ 85%, normal arterial blood gas values, but a V_E/V_{CO2} mismatch, we hypothesize the mice are cycling between hypoxemia/hypercapnia and hypocapnia.

Although 1 h of pulse oximetry revealed differences for oxygen saturation, a single arterial blood sample showed similar P_{aO2} and P_{aCO2} between WT and Ts mice. The blood sample is one point in time while mice are resting quietly in their cage. It is possible that arterial blood gases are always maintained during quiescence in these mice. However, another alternative is that we did not take enough samples over time to determine if P_{aO2} and P_{aCO2} are cycling. Future experiments to quantify oxygen and carbon dioxide levels across time and activity levels are warranted. To our knowledge, the only way to test CO_2 over time in conscious mice would be multiple blood samples, which is incredibly challenging due to their small blood volume. However, end tidal or transcutaneous CO_2 experiments could be investigated in individuals with Ds, as Fan et al. have observed higher CO_2 levels during sleep.[65] In Ts65Dn, perhaps more pulse oximetry experiments are a reasonable way to identify changes in oxygen saturation during various intensities of activity and across the light and dark cycles. It is noninvasive and can be used over multiple time points throughout development. Das et al.[31] did find more oxygen desaturations in the dark cycle vs. the light cycle in Ts65Dn, suggesting more active mice are prone to a higher number of desaturations. While these data point to a contributing mechanism driving reduced V_{O2} and exercise capacity in Ds, it leaves more questions for what mechanisms are causing the high incidence of sleep apnea in this population. It is possible that CO_2 sensing is more likely to contribute to sleep apnea, but potential reduced oxygen delivery is contributing more to activities of daily living.

Lower Hb and Hct levels in Ts65Dn would result in lower oxygen content of arterial blood. These lower Hb and Hct are consistent with a report in humans[69,70] and a previous report in Ts65Dn mice.[71] Mechanisms leading to lower Hb and Hct in Ts65Dn could include inflammation[72] and low iron availability to developing erythrocytes.[73,74] Inflammatory mediators, particularly, IL-6, induce liver hepcidin expression via activation of STAT3.[75] Hepcidin is a peptide hormone that binds to ferroportin, the only known iron export protein, causing its cellular internalization and degradation.[76] Our working hypothesis is an increased IL-6 drives an increase in hepcidin synthesis that results in tissue iron accumulation and reduced plasma iron, which could contribute to lower Hb and Hct levels. This postulate is supported by findings of lower plasma iron,[73,74] elevated IL-6,[72,74] and hepcidin[74] in Ds individuals compared to controls, along with greater brain iron levels obtained from postmortem brain sections.[74] Functionally, a lower Hb level would reduce the amount of oxygen delivered to the tissues and lower Hct could increase hypoxic pulmonary vasoconstriction.[77] Despite the lack of difference in arterial P_{aO2} between groups, our data are consistent with a previous report showing increased oxygen desaturations in Ts65Dn mice during the dark, or active cycle.[31] Collectively, lower Hb and Hct levels combined with elevated desaturations are likely to hinder O_2 delivery to tissues and may be a contributing factor in the reduced exercise capacity of individuals with Ds. However, Das et al. observed a reduction of desaturations in Ts65Dn following treadmill exercise; oxygen saturation is unknown *during* exercise in Ts65Dn. We should also not rule out a reduced Hct potentially influencing the buffering capacity in Ts65Dn and Ds. The mechanisms resulting in reduced Hb and Hct in Ds and their physiological outcomes represent an area of research that is virtually unexplored at the present time.

To complement our hematological data in Ts65Dn, we also compared data from a retrospective medical record review. These comparisons identify the relative risk of anemia is higher in Ds compared to the controls, supporting the lower Hb and Hct data in Ts65Dn. Additionally, we quantified the relative risk in those with sleep apnea and observed elevated relative risk for nutritional and aplastic and other anemias, but not hemolytic anemia in this cohort. Overall, our hypothesis is that lower Hb and Hct likely contribute to reduced activities of daily living in Ds, but that sleep apnea may be more influenced by alterations in CO_2 sensing or motor output in response to changing CO_2 levels. Although it is possible that both mechanisms contribute to sleep apnea and active lifestyles in Ds, more research is warranted to improve the lives of individuals with Ds.

While we uncovered breathing differences with a neural mechanism, we also explored a possible muscle component. Eupneic EMG, in-vitro muscle function and histological analysis revealed no differences in the diaphragm of Ts65Dn and WT mice. This finding was somewhat surprising, as we have

previously observed a reduced functional recovery from fatiguing contractions in the soleus muscle of Ts65Dn, and others have reported reduced CSA of quadriceps and posterior digastric skeletal muscle.[78,79] Additionally, there are structural and metabolic links supporting accelerated aging in limb musculature of Ts65Dn.[80] The diaphragm is a mixed skeletal muscle of multiple fiber types and is chronically active, which may confer some resistance to fiber type shifts and/or weakness during air breathing. Although diaphragm fiber types would not be expected to be equally active during quiet breathing, the more active type I/IIa fiber populations were the most prevalent fiber types. Additionally, the similar pattern of augmented breaths between the groups may have preserved the fast twitch fiber populations.

Ds patients are also prone to skeletal, ligament, and tendon deficiencies,[81–83] resulting in a biomechanical disadvantage, which likely impact longitudinal muscles to a greater degree than diaphragm. Future studies could investigate in-situ muscle contraction of limb or upper airway muscles to study intact muscle and tendons, and neural contraction of the musculature. Upper airway muscles are vital to maintaining a patent airway, particularly with higher force behaviors such as cough and sigh. Decreased neural input to the respiratory muscles may also limit the efficacy of cough and sigh, which are important to clearing the airways. Since one third of all deaths in Ds are attributed to respiratory infections,[10–12] it is important to understand any contributions that may hinder clearance of the airways. Pharyngeal collapse[84] and pharyngeal dysphagia[85] occur in Ds, and are often not improved by removing tonsil and adenoid obstructions, suggesting upper airway muscles are an important link to understanding respiratory physiology in this population.

Limitations

We investigated male Ts65Dn as a model of Ds. Ts65Dn is a well-accepted mouse model that triplicates > 50% of the genes that are also triplicated in Ds, and virtually all of the genes in the Ds critical region. However, some genes that contribute to the Ds phenotype may not be triplicated in Ts65Dn and could confound results. Many aspects of the respiratory phenotype observed in Ds patients were present in Ts65Dn mice, so we posit this model is an adequate and faithful representation of the Ds respiratory phenotype. A limitation is that we studied only male mice. Future investigations should include both male and female mice to understand the physiology of both sexes in Ds. The medical record review includes both male and female patients. Additionally, mice were tested in the light, or less active cycle. It will be important to investigate mice across both the light and dark cycles,[34] particularly with regards to the prevalence of sleep apnea (light cycle) and reduced exercise capacity (dark cycle) in Ds. Lastly, while we have initial mechanistic data showing a CO_2 sensing or motor output deficit, a shortcoming is the lack of insight regarding cellular and molecular changes at the carotid body, C_3–C_5 of the spinal cord, the neuromuscular junction, and/or at the brainstem.

Conclusions

For the first time, we show that Ts65Dn mice have an altered pattern of breathing and represent a potential model for future investigations of respiratory physiology in Ds. At rest, Ts65Dn mice have more apneas and oxygen desaturations along with reduced V_T/T_i. Therefore, these mice are experiencing intermittent hypoxemias throughout their lifetime. There was an attenuated response to hypercapnia in Ts65Dn vs. WT, suggesting a CO_2 sensing or motor output deficit. Arterial blood sampling in resting mice was normal, although hemoglobin concentration and hematocrit levels were lower in Ts65Dn compared to WT mice, which likely contributes to hypoxemias in active mice. We also performed a retrospective medical record review and determined the relative risk of anemia is higher in Ds and remains higher for nutritional anemia, and aplastic and other anemias in those individuals with Ds and sleep apnea. Diaphragm histology, in-vitro muscle function, and eupneic EMG were not different between strains. A neural mechanism, but not a diaphragmatic muscular component, contributes to breathing differences in Ts65Dn and by clinical correlate, Ds.

Acknowledgments

We thank Dr. Jeramia Ory for creating the graphical abstract.

Funding

This work was funded by 1R15 HD076379, 3R15 HD076379-S1, 3R15 HD076379-S2, 1R21 HD099573, and 1R15 AG077421.

Conflict of Interest Statement

None of the authors has any conflict of interest.

Data Availability

The data underlying this article are available in the article.

References

1. Egan JF, Benn PA, Zelop CM, Bolnick A, Gianferrari E, Borgida AF. Down syndrome births in the United States from 1989 to 2001. *Am J Obstet Gynecol* 2004;**191**(3):1044–1048.
2. Shin M, Besser LM, Kucik JE, et al. Prevalence of Down syndrome among children and adolescents in 10 regions of the United States. *Pediatrics* 2009;**124**(6):1565–1571.
3. Birth defects surveillance data from selected states, 1998–2002. *Birth Defect Res A* 2005;**73**(10):758–853.
4. Survey of Income and Program Participation. 2006.
5. Lane SBaDL , ed. *The Development of Intelligence*. New York, NY: Holt, Rinehart and Winston, 1985.
6. Lott IT, Dierssen M. Cognitive deficits and associated neurological complications in individuals with Down's syndrome. *Lancet Neurol* 2010;**9**(6):623–633.
7. McGrath RJ, Stransky ML, Cooley WC, Moeschler JB. National profile of children with Down syndrome: disease burden, access to care, and family impact. *J Pediatr* 2011;**159**(4):535–540.e2.
8. Hilton JM, Fitzgerald DA, Cooper DM. Respiratory morbidity of hospitalized children with trisomy 21. *J Paediatr Child Health* 1999;**35**(4):383–386.
9. Uppal H, Chandran S, Potluri R. Risk factors for mortality in Down syndrome. *J Intellect Disabil Res* 2015;**59**(9):873–881.
10. Colvin KL, Yeager ME. What people with Down Syndrome can teach us about cardiopulmonary disease. *Eur Respir Rev* 2017;**26**(143):160098.
11. Motegi N, Yamaoka Y, Moriichi A, Morisaki N. Causes of death in patients with Down syndrome in 2014–2016: a population study in Japan. *Am J Med Genet A* 2022;**188**(1):224–236.

12. Zhu JL, Hasle H, Correa A, et al. Survival among people with Down syndrome: a nationwide population-based study in Denmark. *Genet Med* 2013;**15**(1):64–69.
13. Bull MJ. Pulmonary complications and chronic conditions of Down syndrome during childhood: an agenda for clinical care and research. *J Pediatr* 2011;**158**(2):178–179.
14. McDowell KM, Craven DI. Pulmonary complications of Down syndrome during childhood. *J Pediatr* 2011;**158**(2):319–325.
15. Uong EC, McDonough JM, Tayag-Kier CE, et al. Magnetic resonance imaging of the upper airway in children with Down syndrome. *Am J Respir Crit Care Med* 2001;**163**(3):731–736.
16. de Jong AL, Sulek M, Nihill M, Duncan NO, Friedman EM. Tenuous airway in children with trisomy 21. *Laryngoscope* 1997;**107**(3):345–350.
17. Krahn KN, Nagraj VP, McCulloch MA, Zimmet AM, Fairchild KD. Hypoxemia in infants with trisomy 21 in the neonatal intensive care unit. *J Perinatol* 2021;**41**(6):1448–1453.
18. da Silva VZ, de Franca Barros J, de Azevedo M, de Godoy JR, Arena R, Cipriano G, Jr. Bone mineral density and respiratory muscle strength in male individuals with mental retardation (with and without Down syndrome). *Res Dev Disabil* 2010;**31**(6):1585–1589.
19. Laibsirinon SJN. Pulmonary function and chest expansion in Thai boys with Down syndrome. *Thammasat Med J* 2012;**12**:(2)269–276.
20. Ricoy J, Rodriguez-Nunez N, Alvarez-Dobano JM, Toubes ME, Riveiro V, Valdes L. Diaphragmatic dysfunction. *Pulmonol* 2019;**25**(4):223–235.
21. Fernhall B, Mendonca GV, Baynard T. Reduced work capacity in individuals with Down syndrome: a consequence of autonomic dysfunction? *Exerc Sport Sci Rev* 2013;**41**(3):138–147.
22. Oviedo GR, Garcia-Retortillo S, Carbo-Carrete M, et al. Cardiorespiratory coordination during exercise in adults with Down syndrome. *Front Physiol* 2021;**12**:704062.
23. Rosen D. Management of obstructive sleep apnea associated with Down syndrome and other craniofacial dysmorphologies. *Curr Opin Pulm Med* 2011;**17**(6):431–436.
24. Merrell JA, Shott SR. OSAS in Down syndrome: T&A versus T&A plus lateral pharyngoplasty. *Int J Pediatr Otorhinolaryngol* 2007;**71**(8):1197–1203.
25. Ravutha Gounden M, Chawla JK. Management of residual OSA post adenotonsillectomy in children with Down syndrome: a systematic review. *Int J Pediatr Otorhinolaryngol* 2022;**152**:110966.
26. Ferri R, Curzi-Dascalova L, Del Gracco S, Elia M, Musumeci SA, Stefanini MC. Respiratory patterns during sleep in Down's syndrome:importance of central apnoeas. *J Sleep Res* 1997;**6**(2):134–141.
27. Pastore E, Marino B, Calzolari A, Digilio MC, Giannotti A, Turchetta A. Clinical and cardiorespiratory assessment in children with Down syndrome without congenital heart disease. *Arch Pediatr Adolesc Med* 2000;**154**(4):408–410.
28. Davisson MT, Schmidt C, Akeson EC. Segmental trisomy of murine chromosome 16: a new model system for studying Down syndrome. *Prog Clin Biol Res* 1990;**360**:263–280. https://pubmed.ncbi.nlm.nih.gov/2147289/.
29. Vacano GN, Duval N, Patterson D. The use of mouse models for understanding the biology of down syndrome and aging. *Curr Gerontol Geriatr Res* 2012;**2012**:717315.
30. Costa AC. On the promise of pharmacotherapies targeted at cognitive and neurodegenerative components of Down syndrome. *Dev Neurosci* 2011;**33**(5):414–427.
31. Das D, Medina B, Baktir MA, et al. Increased incidence of intermittent hypoxemia in the Ts65Dn mouse model of Down syndrome. *Neurosci Lett* 2015;**604**:91–96.
32. Costa AC, Stasko MR, Schmidt C, Davisson MT. Behavioral validation of the Ts65Dn mouse model for Down syndrome of a genetic background free of the retinal degeneration mutation Pde6b(rd1). *Behav Brain Res* 2010;**206**(1):52–62.
33. Reinholdt LG, Ding Y, Gilbert GJ, et al. Molecular characterization of the translocation breakpoints in the Down syndrome mouse model Ts65Dn. *Mamm Genome* 2011;**22**(11–12):685–691.
34. Receno CN, Eassa BE, Cunningham CM, DeRuisseau LR. Young and middle-aged mouse breathing behavior during the light and dark cycles. *Physiol Rep* 2019;**7**(8):e14060.
35. Shoji H, Takao K, Hattori S, Miyakawa T. Age-related changes in behavior in C57BL/6 J mice from young adulthood to middle age. *Mol Brain* 2016;**9**(1):11.
36. Yanai S, Endo S. Functional aging in male C57BL/6 J mice across the life-span: a systematic behavioral analysis of motor, emotional, and memory function to define an aging phenotype. *Front Aging Neurosci* 2021;**13**:697621.
37. Loeven AM, Receno CN, Cunningham CM, DeRuisseau LR. Arterial blood sampling in male CD-1 and C57BL/6 J mice with 1% isoflurane is similar to awake mice. *J Appl Physiol* 2018;**125**(6):1749–1759.
38. Drorbaugh JE, Fenn WO. A barometric method for measuring ventilation in newborn infants. *Pediatrics* 1955;**16**(1):81–87.
39. Receno CN, Glausen TG, DeRuisseau LR. Saline as a vehicle control does not alter ventilation in male CD-1 mice. *Physiol Rep* 2018;**6**(10):e13702.
40. Receno CN, Cunningham CM, Eassa BE, Purdy R, DeRuisseau LR. Method to obtain pattern of breathing in senescent mice through unrestrained barometric plethysmography. *J Vis Exp* 2020;**Apr 28**:(158).
41. Seven YB, Nichols NL, Kelly MN, Hobson OR, Satriotomo I, Mitchell GS. Compensatory plasticity in diaphragm and intercostal muscle utilization in a rat model of ALS. *Exp Neurol* 2018;**299**(Pt A):148–156.
42. Mantilla CB, Seven YB, Zhan WZ, Sieck GC. Diaphragm motor unit recruitment in rats. *Respir Physiol Neurobiol* 2010;**173**(1):101–106.
43. Staib JL, Swoap SJ, Powers SK. Diaphragm contractile dysfunction in MyoD gene-inactivated mice. *Am J Physiol-Regul, Integr Comp Physiol* 2002;**283**(3):R583–R590.
44. McClung JM, Deruisseau KC, Whidden MA, et al. Overexpression of antioxidant enzymes in diaphragm muscle does not alter contraction-induced fatigue or recovery. *Exp Physiol* 2010;**95**(1):222–231.
45. Kavazis AN, DeRuisseau KC, Gordon DM. The senescent rat diaphragm does not exhibit age-related changes in caspase activities, DNA fragmentation, or myonuclear domain. *Eur J Appl Physiol* 2012;**112**(12):3983–3990.
46. Kavazis AN, DeRuisseau KC, McClung JM, et al. Diaphragmatic proteasome function is maintained in the ageing Fisher 344 rat. *Exp Physiol*. 2007;**92**(5):895–901.
47. Ramsey HG. *Functional Data Analysis with R and MATLAB*. New York, NY: Springer, 2009.
48. Eldridge FL. Relationship between phrenic nerve activity and ventilation. *Am J Physiol* 1971;**221**(2):535–543.
49. Davis EM, O'Donnell CP. Rodent models of sleep apnea. *Respir Physiol Neurobiol* 2013;**188**(3):355–361.
50. Hernandez AB, Kirkness JP, Smith PL, et al. Novel whole body plethysmography system for the continuous

characterization of sleep and breathing in a mouse. *J Appl Physiol* 2012;**112**(4):671–680.
51. Barton ER, Wang BJ, Brisson BK, Sweeney HL. Diaphragm displays early and progressive functional deficits in dysferlin-deficient mice. *Muscle Nerve* 2010;**42**(1):22–29.
52. Hakim CH, Lessa TB, Jenkins GJ, Yang NN, Ambrosio CE, Duan D. An improved method for studying mouse diaphragm function. *Sci Rep* 2019;**9**(1):19453.
53. Smuder AJ, Roberts BM, Wiggs MP, et al. Pharmacological targeting of mitochondrial function and reactive oxygen species production prevents colon 26 cancer-induced cardiorespiratory muscle weakness. *Oncotarget* 2020;**11**(38):3502–3514.
54. Nagahisa H, Okabe K, Iuchi Y, Fujii J, Miyata H. Characteristics of skeletal muscle fibers of SOD1 knockout mice. *Oxid Med Cell Long* 2016;**2016**:29345970.
55. Messa GAM, Piasecki M, Hill C, McPhee JS, Tallis J, Degens H. Morphological alterations of mouse skeletal muscles during early ageing are muscle specific. *Exp Gerontol* 2019;**125**:110684.
56. Li LF, Yu CC, Wu HP, et al. Reduction in ventilation-induced diaphragmatic mitochondrial injury through hypoxia-inducible factor 1α in a Murine endotoxemia model. *Int J Mol Sci* 2022;**23**(3):1083.
57. Burns DP, Roy A, Lucking EF, et al. Sensorimotor control of breathing in the *mdx* mouse model of Duchenne muscular dystrophy. *J Physiol* 2017;**595**(21):6653–6672.
58. Fogarty MJ, Brandenburg JE, Zhan WZ, Sieck GC. Diaphragm muscle function in a mouse model of early-onset spasticity. *J Appl Physiol* 2022;**133**(1):60–68.
59. Gregorevic P, Plant DR, Leeding KS, Bach LA, Lynch GS. Improved contractile function of the mdx dystrophic mouse diaphragm muscle after insulin-like growth factor-I administration. *Am J Pathol* 2002;**161**(6):2263–2272.
60. Richard N, Beydon N, Berdah L, Corvol H, Aubertin G, Taytard J. Nocturnal hypoventilation in Down syndrome children with or without sleep apnea. *Pediatr Pulmonol* 2020;**55**(5):1246–1253.
61. Coverstone AM, Bird M, Sicard M, et al. Overnight pulse oximetry for evaluation of sleep apnea among children with trisomy 21. *J Clin Sleep Med* 2014;**10**(12):1309–1315.
62. Chicoine B, Rivelli A, Fitzpatrick V, Chicoine L, Jia G, Rzhetsky A. Prevalence of common disease conditions in a large cohort of individuals with Down syndrome in the United States. *J Patient Cent Res Rev* 2021;**8**(2):86–97.
63. Chen CC, Spano G, Edgin JO. The impact of sleep disruption on executive function in Down syndrome. *Res Dev Disabil* 2013;**34**(6):2033–2039.
64. Breslin J, Spano G, Bootzin R, Anand P, Nadel L, Edgin J. Obstructive sleep apnea syndrome and cognition in Down syndrome. *Develop Med Child Neuro* 2014;**56**(7):657–664.
65. Fan Z, Ahn M, Roth HL, Li L, Vaughn BV. Sleep apnea and hypoventilation in patients with Down syndrome: analysis of 144 polysomnogram studies. *Children* 2017;**4**(7):55.
66. Siriwardhana LS, Nixon GM, Davey MJ, et al. Children with down syndrome and sleep disordered breathing display impairments in ventilatory control. *Sleep Med* 2021;**77**:161–169.
67. Boonman AJN, Schroeder EC, Hopman MTE, Fernhall BO, Hilgenkamp TIM. Cardiopulmonary profile of individuals with intellectual disability. *Med Sci Sports Exerc* 2019;**51**(9):1802–1808.
68. Hendrix JA, Amon A, Abbeduto L, et al. Opportunities, barriers, and recommendations in Down syndrome research. *TRD* 2021;**5**(3–4):99–129.
69. Mittal S, Boan AD, Pereira-Smith S, LaRosa A. Screening for anemia in children with Down syndrome. *J Dev Behav Pediatr* 2020;**41**(2):141–144.
70. Tenenbaum A, Malkiel S, Wexler ID, Levy-Khademi F, Revel-Vilk S, Stepensky P. Anemia in children with down syndrome. *Int J Pediatr* 2011;**2011**:813541.
71. Kirsammer G, Jilani S, Liu H, et al. Highly penetrant myeloproliferative disease in the Ts65Dn mouse model of Down syndrome. *Blood* 2008;**111**(2):767–775.
72. Huggard D, Kelly L, Ryan E, et al. Increased systemic inflammation in children with Down syndrome. *Cytokine* 2020;**March**:154938.
73. Anneren G, Gebre-Medhin M. Trace elements and transport proteins in serum of children with Down syndrome and of healthy siblings living in the same environment. *Hum Nutr Clin Nutr* 1987;**41**(4):291–299.
74. Raha AA, Ghaffari SD, Henderson J, et al. Hepcidin increases cytokines in Alzheimer's disease and Down's Syndrome dementia: implication of impaired iron homeostasis in neuroinflammation. *Front Aging Neurosci* 2021;**13**:653591.
75. Verga Falzacappa MV, Vujic Spasic M, Kessler R, Stolte J, Hentze MW, Muckenthaler MU. STAT3 mediates hepatic hepcidin expression and its inflammatory stimulation. *Blood* 2007;**109**(1):353–358.
76. Nemeth E, Tuttle MS, Powelson J, et al. Hepcidin regulates cellular iron efflux by binding to ferroportin and inducing its internalization. *Science* 2004;**306**(5704):2090–2093.
77. Stembridge M, Hoiland RL, Williams AM, et al. The influence of hemoconcentration on hypoxic pulmonary vasoconstriction in acute, prolonged, and lifelong hypoxemia. *Am J Physiol Heart Circ Physiol* 2021;**321**(4):H738–H747.
78. Glass TJ, Connor NP. Digastric muscle phenotypes of the Ts65Dn mouse model of Down syndrome. *PLoS One* 2016;**11**(6):e0158008.
79. Cisterna B, Costanzo M, Scherini E, Zancanaro C, Malatesta M. Ultrastructural features of skeletal muscle in adult and aging Ts65Dn mice, a murine model of Down syndrome. *Muscles Ligaments Tendons J* 2013;**3**(4):287–294.
80. Cisterna B, Sobolev AP, Costanzo M, Malatesta M, Zancanaro C. Combined microscopic and metabolomic approach to characterize the skeletal muscle fiber of the Ts65Dn mouse, a model of Down syndrome. *Microsc Microanal* 2020;**26**(5):1014–1023.
81. Valle MS, Casabona A, Micale M, Cioni M. Relationships between muscle architecture of rectus femoris and functional parameters of knee motion in adults with Down syndrome. *Biomed Res Int* 2016;**2016**:7546179.
82. Corsi C, Cimolin V, Capodaglio P, Condoluci C, Galli M. A biomechanical study of gait initiation in Down syndrome. *BMC Neurol* 2019;**19**(1):66.
83. Carfi A, Liperoti R, Fusco D, et al. Bone mineral density in adults with Down syndrome. *Osteoporos Int* 2017;**28**(10):2929–2934.
84. Fung E, Witmans M, Ghosh M, Cave D, El-Hakim H. Upper airway findings in children with Down syndrome on sleep nasopharyngoscopy: case-control study. *J Otolaryngol Head Neck Surg* 2012;**41**(2):138–144.
85. O'Neill AC, Richter GT. Pharyngeal dysphagia in children with Down syndrome. *Otolaryngol—Head Neck Surg* 2013;**149**(1):146–150.

Submitted: 11 August 2023; **Revised:** 29 September 2023; **Accepted:** 3 October 2023